Plasma-assisted CO_2 conversion in a gliding arc discharge: Improving performance by optimizing the reactor design

Li Li[a], Hao Zhang[a,*], Xiaodong Li[a], Xiangzhi Kong[a], Ruiyang Xu[a], Kangrou Tay[a], Xin Tu[b,*]

[a] *State Key Laboratory of Clean Energy Utilization, Zhejiang University, Hangzhou 310027, China*

[b] *Department of Electrical Engineering and Electronics, University of Liverpool, Liverpool L69 3GJ, UK*

Abstract:

In this paper, a gliding arc discharge (GAD) is investigated for CO_2 decomposition, with particular efforts directed toward improving the performance by optimizing the reactor design. The effects of various parameters, e.g., gas flow rate, configuration of the injector nozzle, and structure of the quartz cover, on the CO_2 conversion and energy efficiency are investigated. The results indicate that the variation profiles of CO_2 conversion upon rising flow rate can be clearly be divided into two patterns: Pattern A with outlet gas temperature > 440 ^oC and Pattern B with outlet gas temperature < 440 ^oC. The CO_2 conversion rises in Pattern A but decreases in Pattern B with the increase in flow rate. The relatively high temperature in Pattern A is negatively correlated with CO_2 conversion because it can stimulate the recombination of CO and O, which leads to the increase in CO_2 conversion with increasing flow rate (and decreasing gas temperature). A smaller injector nozzle diameter (1.0 mm) exhibits a better performance in terms of both CO_2 conversion and energy efficiency under most of the conditions studied, and a longer distance between the injector nozzle and electrodes is beneficial to the CO_2 conversion at relatively high flow rates (⩾ 4 L/min). A quadrangular reactor cover was proved to have a better space utilization and a higher fraction of gas treatment by plasma, which can ensure a more adequate contact between the injected gas and plasma, and thus a better performance. The optimum conditions are: flow rate = 3 L/min, nozzle diameter = 1.0 mm, distance between injector nozzle and electrodes = 5.0 mm, and a quadrangular cover, under which CO_2 conversion and energy efficiency up to 11.1% and 20.7% can be achieved. Compared to other typical non-thermal plasmas, such as dielectric barrier discharge and corona discharge, GAD shows a

significantly higher energy efficiency along with a flow rate that is an order of magnitude higher.

Keywords: CO_2 decomposition, gliding arc discharge, flow rate, reactor design, gas flow field

1 Introduction

Each year, human activities result in carbon emission of up to 7 Gt into the earth's atmosphere, a large portion of which is in the form of gaseous CO_2 [1]. The concentration of atmospheric CO_2 has reached 400 ppm, the highest level that has ever been recorded in the past 800,000 years [2],[3]. It is clear that increasing anthropogenic emission of greenhouse gases is leading to severe global climate change, thus motivating efforts to develop effective strategies for mitigation or valorization of CO_2. In this regard, three major strategies have been proposed: boosting the use of clean and renewable energy, improving the energy utilization efficiency, and carbon capture, utilization, and storage (CCUS) [4].

As one of the CCUS routes, direct decomposition of CO_2 has attracted particular interest, because it can convert the greenhouse gas into value-added CO, a product that can serve not only as a fuel but also as a widely used chemical feedstock [5][6]. However, CO_2 is a highly stable molecule and its dissociation requires a large amount of activation energy in traditional thermal processes (Eq. (1)) [7].

$$CO_2 \rightarrow CO + \frac{1}{2}O_2 \qquad \Delta H = 280 \text{ kJ/mol} \tag{1}$$

Thermodynamic equilibrium calculation of CO_2 conversion shows that CO_2 starts to decompose only near 2000K with a very low conversion rate (< 1%). A reasonable conversion of CO_2 (~60%) can be obtained only at an extraordinarily high temperature of 3000–3500K [6], which leads to a high energy cost thus rendering it undesirable in practical applications.

Non-thermal plasma (NTP) is increasingly considered as one of the promising approaches for CO_2 utilization [8]-[10], because it enables the thermodynamically unfavorable CO_2 activation to occur at a reduced energy cost under mild conditions, i.e., lower temperature and atmospheric pressure. In non-thermal plasmas, the average electron temperature, i.e., the kinetic energy of free electrons typically in electron volts (eV), can be as high as 1–10 eV, giving rise to the generation of a variety of reactive species (e.g., excited species, radicals, ions, and photons) that are responsible for the efficient initiation and propagation of reactions [11]-[12]. Meanwhile, the gas temperature of non-thermal plasmas can be very low (e.g., 200–500 °Cor even room temperature), which ensures a low energy cost due to the reduced heat loss[13]. Because of the unique merits of non-thermal plasmas, they have been widely investigated and applied to a variety of fields, such as material treatment [14]-[15], waste water disposal [16], fuel reforming [10][17], and plasma-aided combustion [18][19], etc.

Among various non-thermal plasmas used for CO_2 activation, gliding arc discharge (GAD) is attracting particular attention because it features the merits of both non-thermal and thermal plasmas [20], enabling it to simultaneously provide high power, good selectivity to chemical processes and high energy efficiency. Traditionally, a GAD reactor consists of two diverging electrodes. The arc is generated in the narrowest electrode gap, and then moves along the electrodes with increasing length due to the pushing force of gas flow. In this way, a discharge zone between the two electrodes can be generated for the plasma chemical reactions [21]. The GAD shows a relatively high electron density of up to 10^{20} m^{-3} [22]. The electron temperature is in the range of 0.9-2 eV (10000 K-23000 K) (typically 1 eV), which is about 5-10 times higher than the gas temperature [22][23]. It is already known that a mean electron temperature of 1 eV is most suitable for the efficient vibrational excitation of CO_2 [24]. In plasmas, the excitation of the asymmetric vibrational mode of CO_2 has been proven to be the most efficient pathway for CO_2 activation [25][26]. The proper electron temperature and relatively high electron density of the GAD plasma can give somewhat more vibrational excitation, indicating that a larger overpopulation of the vibrational states can be reached, and an efficient conversion of CO_2 is achievable in GAD [22][25].

There are still some drawbacks in GAD reactors which limit their energy efficiency. Although the GAD shows a somewhat 3D structure, as demonstrated by Kusano et al.

and Zhu et al. [14][27], the volume of plasma is limited due to the nearly 2D structure of the reactor. In addition, the gas flow speed needed is very high and the volume of the reactant gas flow is significantly larger than the plasma volume, indicating that a large part of the reactant gas cannot pass through the plasma area or pass through it only with a limited residence time. This property leads to a low gas conversion and limited efficiency [11][28]. In short, the small treated fraction is still the major limiting factor for the conversion. In this regard, an improvement in the CO_2 conversion performance of GAD can be clearly expected by optimizing the design of the plasma source, e.g., shape of the cover and diameter of the injector nozzle together with the distance between the nozzle and electrodes. In this way, the gas flow field and the distribution of reactive species (e.g., excited species, radicals, ions, and photons) can be optimized to achieve a more adequate treatment of the reactant gas.

Therefore, this work devotes particular effort to obtaining insights toward improving the CO_2 activation performance in GAD by optimizing the source design. The effects of the diameter of the injector nozzle, the distance between the injector and electrodes as well as the structure of the quartz cover (cylindrical or quadrangular) on the reaction performance of CO_2 decomposition in GAD were investigated. Unlike the cylindrical cover that is commonly used to form the plasma chamber in the literature [29]-[31], a quadrangular cover was designed in this study in order to improve the treatment of the reactant gas by plasma. In addition, the influence of the feed flow rate has also been emphasized, as it was identified as a key parameter affecting plasma chemical reactions, especially in GAD reactors.

2 Experimental setup

The schematic diagram of the experimental setup is shown in Fig. 1. The GAD reactor consists of two knife-shaped electrodes (with a length of 17 mm and base width of 2 mm), a gas nozzle and a quartz cover. The plasma was powered by a customized 10 kV DC power supply (TLP2040, Teslaman). A 40 kΩ resistance was connected in series in the circuit to limit and stabilize the current. The CO_2 reactant gas (purity, 99.9%)

was injected into the reactor via the gas nozzle. A thermocouple thermometer (TM-902C+ WRNK-81530) was placed 80 mm downstream of the electrode tip to measure the temperature of the outlet gas. The concentration of CO_2 was measured in real time with a portable CO_2 analyzer (GXH-3010E1, Huayun Instrument Co.). The other gaseous products were analyzed by a gas chromatograph (GC, GC9790A, Fuli Analytical Instrument Co.) equipped with a thermal conductivity detector (TCD) for the measurement of O_2 and a flame ionization detector (FID) with a catalytic methanation unit for detecting CO.

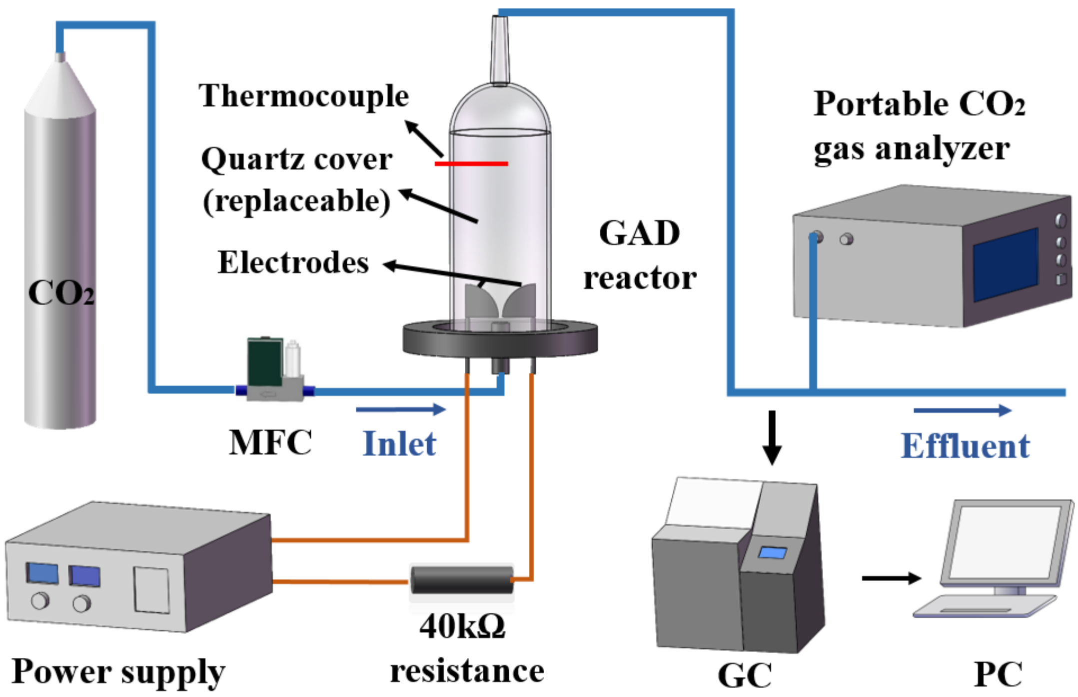

Fig. 1. Schematic diagram of the experimental setup.

Figure 2 shows the configuration of the GAD reactor with different designs for the quartz cover. The cylindrical quartz cover (Fig. 2(a)) is 24 mm in diameter and 120 mm in length. The quadrangular quartz cover (Fig. 2(b1), Fig. 2(b2)) has dimensions of 45×11×120 mm. Other variable parameters in the experiments are shown in Fig. 3, i.e., the distance between the injector nozzle and the electrodes (D) and the diameter of the injector nozzle (Φ).

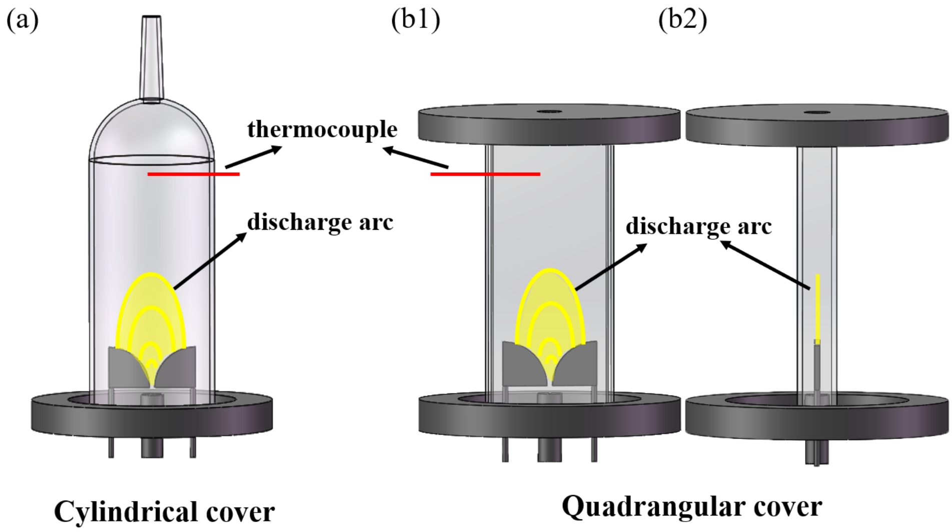

Fig. 2. GAD reactor with different quartz covers.

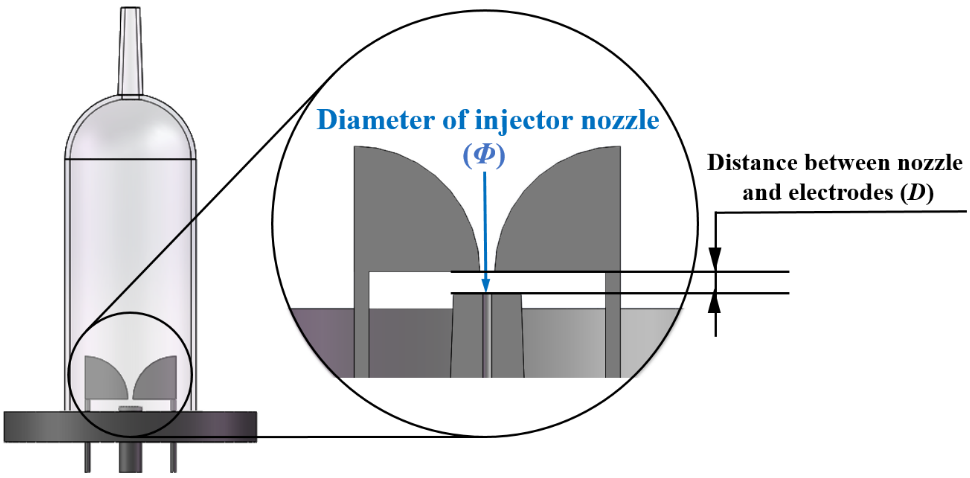

Fig. 3. Configuration of the injector nozzle and electrodes.

The performance of the GAD assisted CO_2 decomposition process is presented mainly in terms of CO_2 conversion C_{CO_2}, carbon balance B_{Carbon} and energy efficiency η, which were defined as:

$$C_{CO_2}(\%)=\frac{\mathrm{CO_2\ converted\ (mol/s)}}{\mathrm{CO_2\ introduced\ (mol/s)}}\times 100 \quad (2)$$

$$B_{Carbon}(\%)=\frac{\mathrm{CO_2\ output\ (mol/s)+\ CO\ produced\ (mol/s)}}{\mathrm{CO_2\ introduced\ (mol/s)}}\times 100\% \quad (3)$$

$$\eta\ (\%)=\frac{CO_2\ \text{converted (mol/s)}\cdot\Delta H\ \text{(J/mol)}}{\text{Power (W)}}\times 100\% \qquad (4)$$

Wherein ΔH is the standard reaction enthalpy and here it is 280 kJ/mol.

Specific energy input (*SEI*) was used to evaluate the energy density, as defined in Eq. (5).

$$SEI\ \text{(kJ/L)}=\frac{\text{Discharge power (W)}}{CO_2\ \text{flow rate (mL/s)}} \qquad (5)$$

3 Results and discussion

3.1 Effect of feed flow rate

In GAD, feed flow rate is an important parameter influencing the dynamic behavior of the discharge, as reported by Zhu et al. [32], therefore its effect is investigated in this part of the study. The feed flow rate was adjusted from 2 to 8 L/min, with a Φ of 1.5 mm and a D of 5.0 mm, using the cylindrical quartz cover.

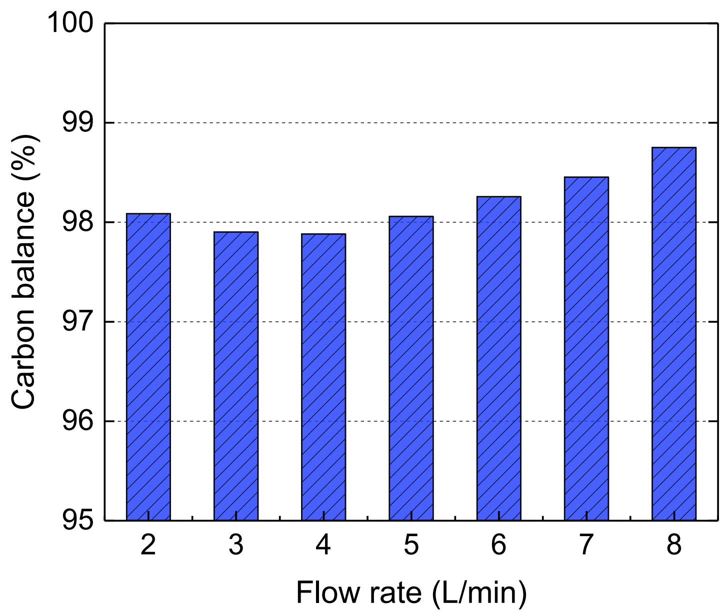

Fig. 4 Carbon balance of the reaction as a function of CO_2 feed flow rate. (cylindrical cover)

The carbon balance of the CO_2 dissociation reaction in the GAD at different feed flow rates is illustrated in Fig. 4. Clearly, the carbon balance reaches almost 100% (ranging from 97.9 to 98.8%) under all the conditions studied. In addition, carbon deposition was not found in the reactor. This indicates that CO is the main product and the major reaction in the GAD assisted CO_2 decomposition is $CO_2 \rightarrow CO + 1/2\ O_2$. Therefore, in the following sections, the CO_2 conversion and energy efficiency will be considered as the main indicators for evaluating the performance of the reaction, without focusing on the selectivity and yield of products.

Figure 5 shows the variation in discharge power and *SEI* with the increasing flow rate. As expected, a continuous decrease of *SEI* is observed due to the increasing amount of feed gas. A higher breakdown power was needed to form an arc discharge at the higher gas flow rate, leading to a higher discharge power with the increasing flow rate [33]. In addition, the increased heat loss with rising flow rate results in the need for a higher discharge power. Figure 6 shows the effect of flow rate on the CO_2 conversion and energy efficiency. With the increase in flow rate, CO_2 conversion first rises to a maximum value of 7.2% at a flow rate of 4 L/min, and then decreases. The energy efficiency continuously rises and tends to reach a limitation after the flow rate is over 6 L/min due to the drop of the CO_2 conversion. The maximum energy efficiency can reach 25.8% at a flow rate of 8 L/min.

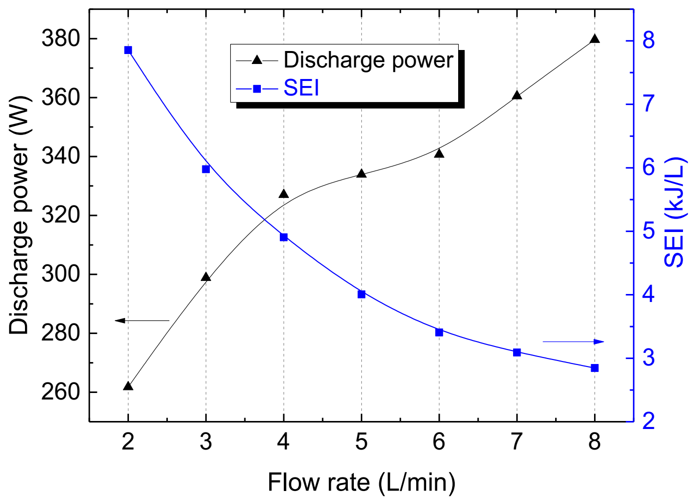

Fig. 5. Effect of gas flow rate on the discharge power and *SEI*. (cylindrical cover)

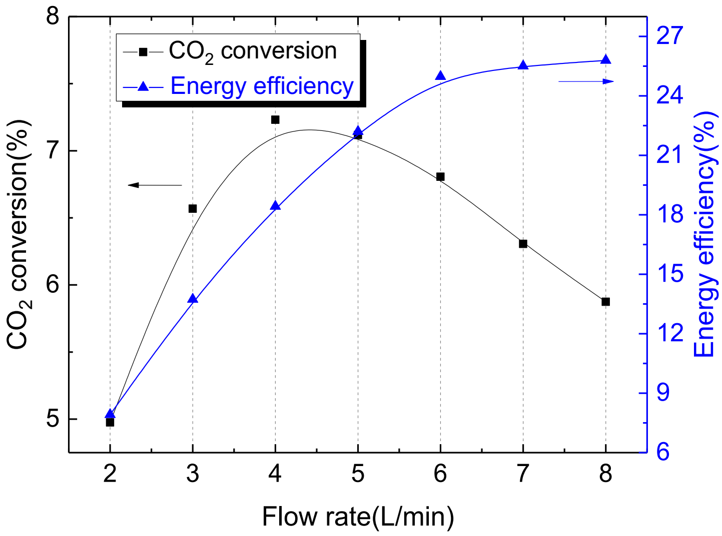

Fig. 6. Effect of gas flow rate on the CO_2 conversion and energy efficiency. (cylindrical cover)

Similar variation tendencies in energy efficiency with feed flow rate can be found in other studies [29][34]. However, the tendency toward CO_2 conversion is surprisingly not in line with other research om the of plasma CO_2 dissociation process, including GAD [29][35], dielectric barrier discharge (DBD) [36]-[38], microhollow cathode discharge [34][39], nanosecond-pulsed discharge [40] and radio-frequency discharge [41]. In these studies, increasing flow rate has a negative effect on the CO_2 conversion, which should be ascribed to the decreased retention time of gas in the plasma and lowered *SEI*.

The somewhat strange phenomenon in CO_2 conversion in this work is probably related to the reaction temperature. The rate coefficient (k) of the reverse reaction of CO_2 dissociation (see Eq. (6), Arrhenius equation) is positively correlated with the gas temperature. The gas temperature in the central area of the GAD plasma can reach 1000 K [22], which is thus high enough to enable the presence of a reverse reaction [42]. To illustrate the role of gas temperature in the GAD CO_2 dissociation process, the time-dependent gas temperature of the outlet gas was detected and plotted in Fig. 7.

$$\mathrm{CO+O} \rightarrow \mathrm{CO_2} \quad k(\mathrm{T}) = 1.7\times10^{-33}\left[\mathrm{cm^6/molecule^2 s}\right]\cdot e^{-12.55[\mathrm{kJ/mole}]/RT} \quad (300\text{ -}2500\mathrm{K}) \quad (6)$$

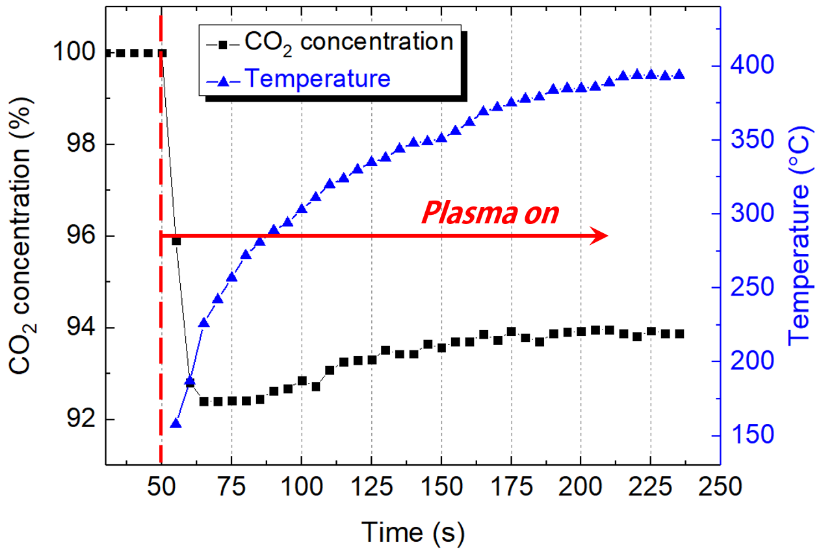

Fig. 7 Time-dependent CO_2 concentration and outlet gas temperature (cylindrical cover, flow rate = 5 L/min, *D* = 10.0 mm, *Φ* = 1.5 mm).

Clearly, the CO_2 concentration has a variation trend similar to the gas temperature, i.e., it increases after the plasma is on (at 50s) and then is stabilized after 3 minutes of operation. It should also be noted that with the increase in feed flow rate (and decrease in gas temperature), the time-dependent variation of online CO_2 concentration was significantly weakened. These phenomena partly manifest the negative effect of high temperature on CO_2 decomposition in the GAD plasma, especially at low feed flow rate. That is similar to the study by Faisal et al., who explained that the conversion of toluene slightly decreases when increasing the temperature as a result of the increasing rate of the recombination reaction of the CO and O radicals [43].

In order to further understand the role of gas temperature under different conditions, the outlet gas temperature (3 mins after plasma is on) and CO_2 conversion are plotted in Fig. 8 with increasing flow rates. Interestingly, a maximum value at a flow rate of around 4.3 L/min in the CO_2 conversion curve is clearly observed, which can divide the variation profile into two patterns, as shown in Fig. 8. The CO_2 conversion increases with increasing gas flow rate in Pattern A; Whereas, after the maximum value, a completely opposite tendency in CO_2 conversion presents in Pattern B. The variation profile of CO_2 conversion with increasing feed flow rate could be the result of several factors, e.g., decreasing *SEI*, decreasing gas temperature as well as decreasing retention time of CO_2 in plasma. Considering the negative effect of high temperature on CO_2 conversion, the drop in gas temperature and the decrease in the retention time are both probably responsible for the enhancement of CO_2 conversion in Pattern A. Meanwhile, from our previous study, an increasing gas flow rate can enhance the vibrational kinetics energy of a rotating gliding arc plasma [44], which could probably vibrationally excite CO_2 to a more efficient pathway and improve the efficiency of CO_2 conversion to some extent. In Pattern B, the negative effect of gas temperature is weakened with decreasing temperature, and thus the CO_2 conversion starts to drop with decreasing retention time and *SEI*.

As indicated in Fig. 8, the outlet gas temperature at the turning point is around 440 ^{o}C. When the results of other typical conditions (see Table 1) in this work are plotted in one figure (see Fig. 9), it is interesting to find that almost the same turning point in the outlet gas temperature (440 ^{o}C) for CO_2 conversion can be observed. These phenomena allow us to make a plausible conclusion that, with increasing gas temperature to a certain value, the negative effect of high temperature starts to dominate the conversion of CO_2.

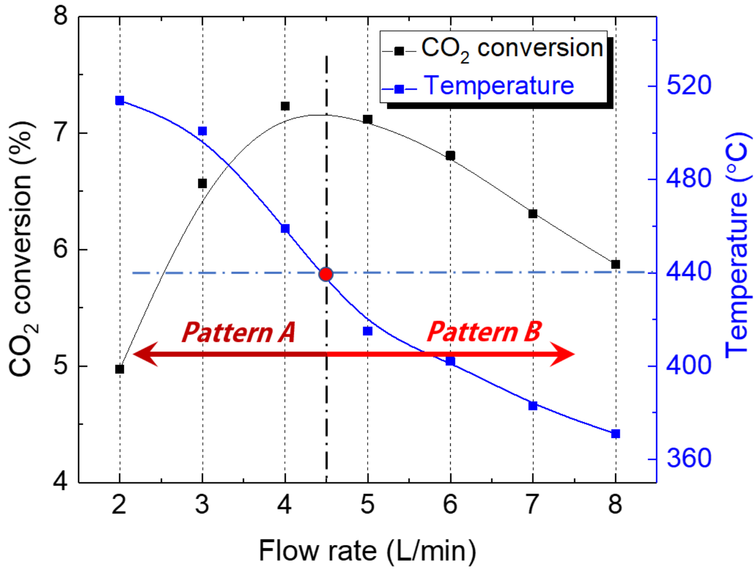

Fig. 8 CO_2 conversion and outlet gas temperature at different flow rates.

(Cylindrical cover)

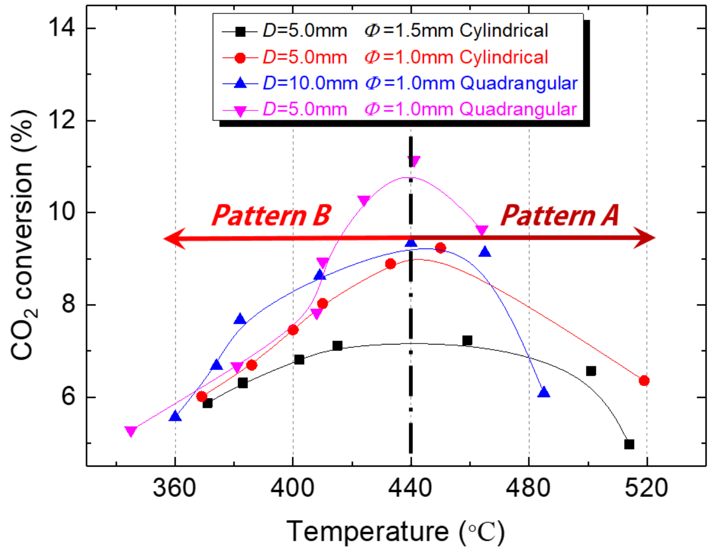

Fig. 9 Relation of the outlet gas temperature and CO_2 conversion under different conditions (see Table 1).

Table 1. Experimental conditions

Experiment	*D* (mm)	*Φ* (mm)	Flow rate (L/min)	Cover shape
(1)	5.0	1.5	2-8	Cylindrical
(2)	5.0	1.0	2-8	Cylindrical
(3)	10.0	1.0	2-8	Quadrangular
(4)	5.0	1.0	2-8	Quadrangular

3.2 Effect of injector nozzle configuration

The configuration of the injector nozzle is an important parameter that can influence the gas flow field and plasma characteristics, and thus the conversion of CO_2. In order to determine the optimized configuration for the injector nozzle, the injector nozzle diameter (*Φ*) and the distance between injector and electrodes (*D*) were adjusted while using the cylindrical quartz cover. The conditions studied in this part are listed in Table 2. CO_2 conversions under different conditions are schematically shown in Fig. 10.

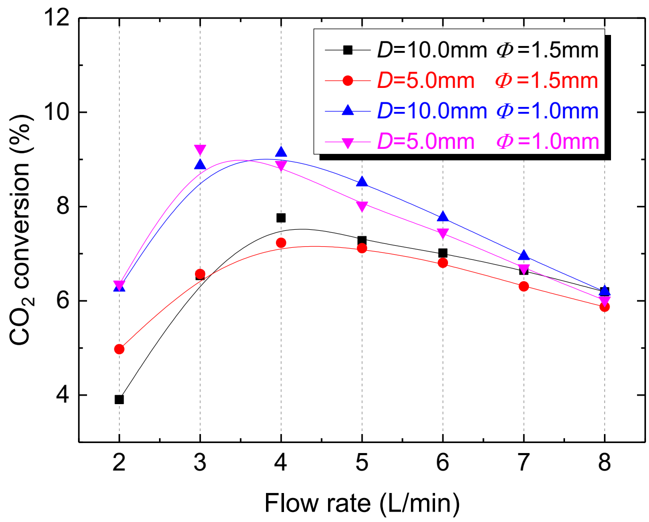

Fig. 10 Effects of *Φ* and *D* on the CO_2 conversion with increasing feed flow rate.

(Cylindrical cover)

Table 2. Experimental conditions

Experiment	*D* (mm)	*Φ* (mm)	Flow rate (L/min)	Cover shape
(5)	10.0	1.5	2-8	Cylindrical
(6)	5.0	1.5	2-8	Cylindrical
(7)	10.0	1.0	2-8	Cylindrical
(8)	5.0	1.0	2-8	Cylindrical

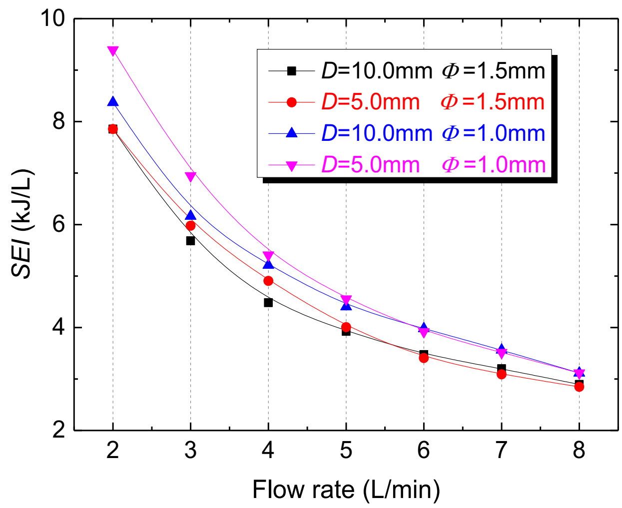

Fig. 11 Effects of *Φ* and *D* on the *SEI* with increasing feed flow rate.

(Cylindrical cover)

As seen from Fig. 10, the four curves with different nozzle configurations show the same trend in variation with increasing feed flow rate. The CO_2 conversion rises when the flow rate is lower than 4 L/min and then decreases when further increasing the flow rate. However, it is obvious that the four curves can be divided into two major categories depending on the Φ. The efficiency of CO_2 conversion with Φ = 1.0 mm is clearly higher in comparison to Φ = 1.5 mm, especially at a gas flow rate $\leqslant$ 7 L/min. Young et al. also reported that a smaller nozzle diameter has a better performance when using a GAD reactor to decompose benzene [45]. A reasonable explanation for this phenomenon is given below. At a fixed flow rate, a smaller nozzle diameter gives rise to a higher gas injection velocity, which ensures a shorter retention time of gas in the plasma. As mentioned earlier, the retention time may play a negative role in the conversion of CO_2, especially at a high gas temperature, due to the recombination reaction of CO and O_2. In this regard, a decreased retention time with smaller Φ is possibly responsible for the higher CO_2 conversion. A phenomenon that can partially manifest this explanation is, decreasing flow rate (and thus increasing gas temperature) results in a larger difference of CO_2 conversion between the results of Φ = 1.0 mm and 1.5 mm, as clearly shown in Fig. 10. Meanwhile, a higher gas injection velocity needs a higher breakdown power to produce a discharge arc [33], as shown from the *SEI* plotted in Fig. 11.

The distance between the electrodes and nozzle does not exhibit any significant impact on the CO_2 conversion, as shown in Fig. 10. Generally, a longer distance leads to a better conversion performance, especially at a high flow rate > 4 L/min.

The optimized results are CO_2 conversion = 9.1% with energy efficiency of 21.9% and flow rate of 4 L/min in experiment (7) and CO_2 conversion = 9.2% with energy efficiency of 16.6% and flow rate of 3 L/min in experiment (8). The former has better energy efficiency due to the higher flow rate.

In summary, the configuration of the nozzle (especially the nozzle diameter) has a significant impact on CO_2 conversion. The optimum conditions for flow rate ≤ 3 L/min are D = 5.0 mm and Φ = 1.0 mm, while for a flow rate of 4 to 8 L/min, D = 10.0 mm and Φ = 1.0 mm show a better performance.

3.3 Effect of quartz cover structure

As mentioned above, the structure of the quartz cover is associated with the gas flow field and distribution of reactive species in the plasma, and is thus important for the efficiency of CO_2 conversion. Two types of covers, i.e., cylindrical and quadrangular ones, were investigated when the D and Φ were fixed at 5.0 mm and 1.5 mm, respectively. Figure 12 and 13 show the variation in CO_2 conversion and energy efficiency with increasing flow rate with different reactor covers, respectively. When using the cylindrical cover, CO_2 conversion rises from 6.4% to a maximum of 9.2% with the flow rate increasing from 2 to 3 L/min, and then drops nearly linearly to 6.0% when further increasing the flow rate from 3 to 8 L/min. The energy efficiency continuously grows from 8.5 to 24.1% but with a gradually slower growth rate with increasing flow rate. For the quadrangular cover, the variation profiles of both the CO_2 conversion and energy efficiency with increasing flow rate are similar to that of the cylindrical cover. The CO_2 conversion increases from 9.6 to 11.1% first and then gradually drops to 5.3%. The energy efficiency increases from 16.1 to 25.2% with flow rate increasing from 2 to 5 L/min, then slightly fluctuates between 23.4 and 25.9%. Interestingly, if the energy efficiency is defined as (lower heating value in the product CO – J/mol) × (CO flow rate – mol/s) / (discharge power in W), the energy efficiency under the conditions of the best CO_2 conversion (flow rate = 3 L/min, Φ = 1.0 mm, D = 5.0 mm, and a quadrangular cover) should be 21.4%.

Clearly, the quadrangular cover exhibits a better performance than the cylindrical cover in terms of both CO_2 conversion and energy efficiency. In the cylindrical cover, a large amount of unreacted gas bypasses the plasma area, causing an inefficient conversion of CO_2. The quadrangular cover can gather the gas forcibly to the central reactive area of the plasma, which enables a better space utilization and thus a higher possibility of the reaction between CO_2 gas and plasma. In addition, the cross section area of the quadrangular cover (4.95 cm^2) is smaller than that of the cylindrical (18.10 cm^2) one, resulting in a higher gas velocity (and lower retention time of gas in the plasma) in the quadrangular cover at the same flow rate. As mentioned above, a lower retention time at a relatively high gas temperature could be helpful toward a higher CO_2 conversion, which is probably also responsible for the better performance of the quadrangular cover. At a lower flow rate, a larger difference in both the CO_2 conversion and energy efficiency between the two covers can be clearly seen, partly manifesting the role of retention time in CO_2 conversion, because the gas temperature decreases with increasing flow rate.

To better understand the effect of the shape of the cover on the gas flow field, the distributions of the gas flow field and gas velocity inside the GAD have been simulated and calculated using COMSOL Multiphysics 5.2 software (three-dimensional laminar flow module), as shown in Fig. 14. Clearly, the gas speed is higher and more injected gases are concentrated in the reaction area when using the quadrangular cover because of the controlled space. Meanwhile, the downstream configuration of the quadrangular cover ensures the formation of a recirculation region (see Fig. 14) that can remarkably increase the fraction of gas treatment by plasma because a large amount of unreacted gas can return to the reaction area for further reaction.

In short, the quadrangular cover shows a better processing efficiency in comparison to the cylindrical cover, especially at a lower flow rate, due to a better space utilization and a higher fraction of gas treatment by the plasma. Therefore, this work provides valuable insights into optimizing a GAD reactor by optimizing the cover structure.

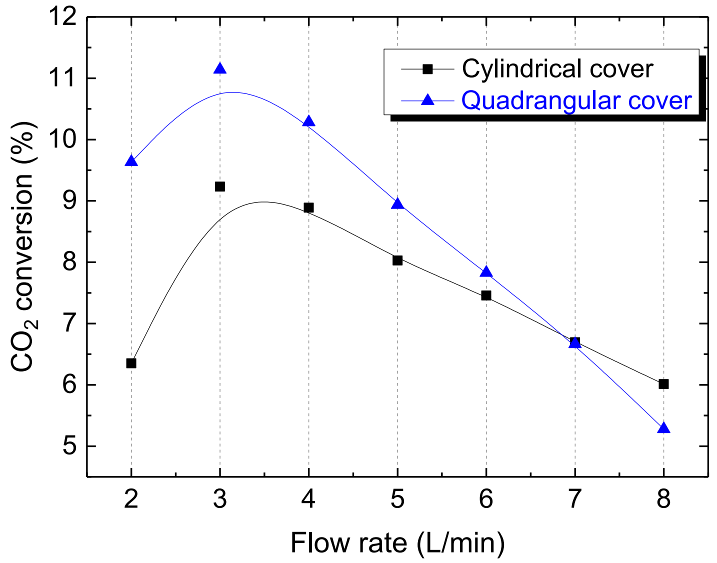

Fig. 12. Effect of quartz cover structure on the CO_2 conversion.

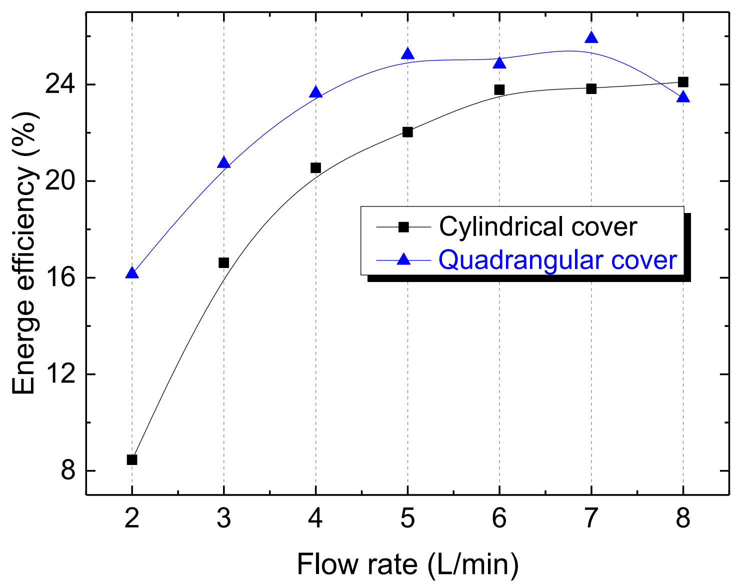

Fig. 13. Effect of quartz cover structure on the energy efficiency.

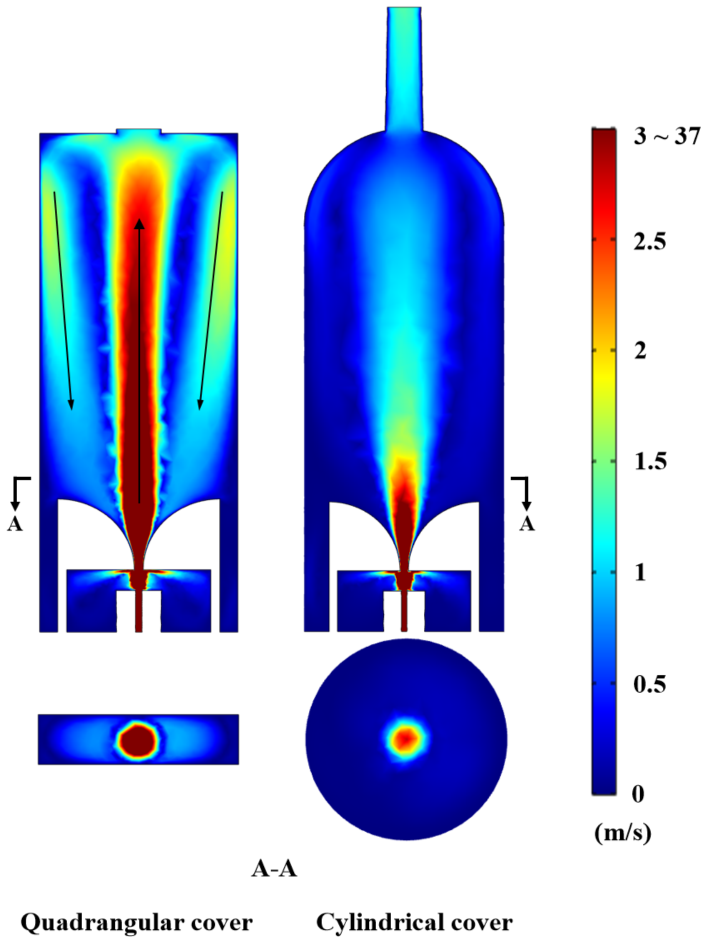

Fig. 14 Simulated contours of gas velocity magnitude of reactor with different covers (flow rate = 5 L/min, *D* = 5.0 mm, *Φ* = 1.5 mm).

3.4 Comparison with other works

In this GAD reactor, a CO_2 conversion of 5.0% to 11.1% and an energy efficiency of up to 26.0% could be achieved. At the optimum conditions, 11.1% of feed CO_2 was decomposed while the energy efficiency was 20.7%. In Table 3, our results are compared with that of other works, such as GAD, DBD, microwave (MW) plasma, nanosecond-pulsed (ns-pulse) discharge and corona discharge. Note that only the optimum values for the conversion and energy efficiency were selected from the literature. The results of the traditional thermal dissociation process are also listed here for comparison.

Table 3 Comparison of the performance of CO_2 dissociation processes among different non-thermal plasmas

Plasma type	Flow rate (mL/min)	CO_2 conversion (%)	Energy efficiency (%)	Ref.
GAD	3000	11.1	20.7	This work
GAD	14000	9.0	18.0	[5]
GAD	850	18.0	-	[29]
GAD	1000	8.6	30.0	[35]
GAD	6500	10.0	20.0	[46]
MW	5000	30.0	40.0	[47]
MW	2200	90.0	10.0	[48]
ns-pulse	120	7.3	11.5	[40]
Corona	90	10.9	1.7	[49]
DBD		24.5	2.4	[37]
DBD	10	35.0	2.0	[50]
DBD	40	12.5	3.5	[51]
DBD	25	27.2	2.8	[52]
DBD	100	25.2	5.3	[53]
Thermal splitting	20	22.0	-	[54]

As shown in Table 3, the optimum CO_2 conversion and energy efficiency were reported using a MW plasma reaching up to 30% and 40%, or 90% and 10%, respectively, at a flow rate of 5000 or 2200 mL/min [47][48]. However, these results were observed only at a low-pressure condition of around 150 mbar, leading to significantly extra energy needed for vacuum supply. This is undoubtedly industrially undesirable. Clearly, DBD has a remarkable CO_2 conversion but with a fairly low energy efficiency of normally $< 5\%$. Both corona discharge and nanosecond-pulsed discharge present a limited performance in CO_2 conversion and energy efficiency. In addition, DBD, nanosecond-pulsed discharge and corona discharge have extremely low flow rates which indicate a poor processing capacity and thus are industrially unfavorable. In general, GAD has a good performance in terms of both CO_2 conversion and energy efficiency. In our work, the CO_2 conversion reached 11.1% and the energy efficiency reached 20.7% while the flow rate reached 3000 mL/min. Not only a favorable efficiency but also a remarkably high processing capacity. It should be noted that in comparison to the conventional means of CO_2 decomposition, like solid-oxide electrolytic cell, where a current efficiency of up to 69% can be obtained [55], the GAD plasma technology shows a relatively low energy efficiency but a remarkably high processing capacity. In addition, the unique properties of non-thermal plasma, e.g., instant on/off, high specific production, low investment and operational cost, operation under atmospheric pressure and low temperature and potential to directly use the electricity produced from intermittent renewable energies (e.g., solar and wind), make it promising for CO_2 decomposition.

Considering the negative effect of high gas temperature (especially at low flow rates) in this GAD plasma, an enhancement in the CO_2 dissociation performance can be expected by cooling the plasma reaction area to inhibit the reverse reaction of CO_2 decomposition. In addition, as previously reported [56][57], the shape and length of the electrodes can also influence the reaction performance in GAD plasma, which is possibly another fruitful direction to improve the CO_2 dissociation performance.

4. Conclusion

A gliding arc discharge (GAD) was investigated in this work for CO_2 decomposition. The influences of flow rate, distance between the injector nozzle and electrodes, diameter of injector nozzle and structure of the quartz cover on the direct dissociation of CO_2 were emphasized, providing insights on the route for improving the performance of a GAD assisted CO_2 activation process by optimizing the source design.

The trend in CO_2 conversion with increasing gas flow rate shows two patterns: Pattern A with flow rate < 4 L/min (outlet gas temperature > 440 ^oC) and Pattern B with flow rate > 4 L/min (outlet gas temperature < 440 ^oC). The CO_2 conversion increases in Pattern A but decreases in Pattern B. With increasing plasma gas temperature to a certain value (at outlet gas temperature of 440 ^oC), the negative effect of high temperature starts to dominate the conversion of CO_2 by stimulating the recombination reaction of CO and O_2. In this case, a longer retention time of gas in the plasma may also provide a negative effect on the CO_2 conversion. The rising CO_2 conversion in Pattern A with increasing flow rate probably results from the decreased gas temperature and retention time.

A smaller injector nozzle diameter of 1.0 mm is more beneficial for CO_2 conversion compared with that of 1.5 mm under most of the conditions studied, because of the lower retention time in the plasma area. The 10 mm distance between the injector nozzle and electrodes shows a better performance in comparison to the 5 mm at relatively high flow rate (flow rate ⩾ 4 L/min).

A quadrangular cover clearly shows a better performance than the traditional cylindrical cover, because of the better space utilization and enhanced fraction of gas treatment by plasma under the optimized gas flow field.

A smaller nozzle diameter of 1.0 mm, a distance between the electrodes and nozzle of 5.0 mm and a flow rate of 3 L/min with a quadrangular cover are suggested to simultaneously obtain a relatively high CO_2 conversion (11.1%) and energy efficiency (20.7%) in the GAD reactor.

Acknowledgements

This work is supported by the National Natural Science Foundation of China (No. 51706204 and No. 51576174) and the China Postdoctoral Science Foundation (No. 2018M630673).

Reference

[1] D. Aaron, C. Tsouris, Separation of CO_2 from flue gas: A review, Sep Sci Technol 40 (2005) 321-348.

[2] R.K. Pachauri, M.R. Allen, V. Barros, J. Broome, W. Cramer, R. Christ, J. Church, L. Clarke, Q. Dahe, P. Dasgupta, Climate change 2014: synthesis Report. Contribution of working groups I, II and III to the fifth assessment report of the intergovernmental panel on climate change, IPCC2014.

[3] D.W. Lea, Palaeoclimate: Climate sensitivity in a warmer world, Nature 518 (2015) 46-47.

[4] B. Smit, A.H.A. Park, G. Gadikota, The grand challenges in carbon capture, utilization, and storage, Front Energy Res 2 (2014) 55.

[5] T. Nunnally, K. Gutsol, A. Rabinovich, A. Fridman, A. Gutsol, A. Kemoun, Dissociation of CO_2 in a low current gliding arc plasmatron, J Phys D Appl Phys 44 (2011) 274009.

[6] D.H. Mei, X.B. Zhu, Y.L. He, J.D. Yan, X. Tu, Plasma-assisted conversion of CO_2 in a dielectric barrier discharge reactor: understanding the effect of packing materials, Plasma Sources Sci T 24 (2015) 015011.

[7] W.Q. Jin, C. Zhang, P. Zhang, Y.Q. Fan, N.P. Xu. Thermal decomposition of carbon dioxide coupled with POM in a membrane reactor, Aiche J 52 (2010) 2545-2550.

[8] D. Ray, R. Saha, S. Ch. DBD plasma assisted CO_2 decomposition: Influence of diluent gases, Catalysts 7 (2017) 244.

[9] D.H. Mei. Plasma-catalytic conversion of greenhouse gas into value-added fuels andchemicals, The University of Liverpool, 2016.

[10] H. Zhang, X.D. Li, F.S. Zhu, K.F. Cen, C.M. Du, X. Tu, Plasma assisted dry reforming of methanol for clean syngas production and high-efficiency CO_2 conversion, Chem Eng J 310 (2017) 144-199.

[11] H. Zhang, F.S. Zhu, X.D. Li, K.F. Cen, C.M. Du, X. Tu, Enhanced hydrogen production by methanol decomposition using a novel rotating gliding arc discharge plasma, Rsc Adv 6 (2016) 12770-12781.

[12] H. Zhang, W.Z. Wang, X.D. Li, L. Han, M. Yan, Y.J Zhong, X. Tu, Plasma activation of methane for hydrogen production in a N_2 rotating gliding arc warm plasma: A chemical kinetics study, Chem Eng J 345 (2018) 67-78.

[13] H. Zhang, L. Li, X.D. Li, et al. Warm plasma activation of CO_2 in a rotating gliding arc discharge reactor, J CO_2 Util 27 (2018) 472-479.

[14] Y. Kusano, B.F. Sørensen, T.L. Andersen, H.L. Toftegaard, F. Leipold, M. Salewski, Z.W. Sun, J.J. Zhu, Z.S. Li, M. Alden, Water-cooled non-thermal gliding arc for adhesion improvement of glass-fibre-reinforced polyester, J Phys D Appl Phys 46 (2013) 135203-135207.

[15] M.P. Srivastava, K. Akira, Carbon dioxide decomposition by plasma methods and application of high energy and high density plasmas in material processing and nanostructures, Trans JWRI 39 (2010) 1.

[16] B. Jiang, Studies on the techniques of coking waste water with pulsed discharge plasma, Industrial Safety and Dust Control, 2005.

[17] T. Paulmier, L. Fulcheri, Use of non-thermal plasma for hydrocarbon reforming,

Chem Eng J 106 (2005) 59-71.
[18] Y.G. Ju, W.T. Sun, Plasma assisted combustion: Dynamics and chemistry, Prog Energ Combust 48 (2015) 21-83.
[19] I.V. Adamovich, W.R. Lempert. Challenges in understanding and predictive model development of plasma-assisted combustion, Plasma Phys Contr F 57 (2015) 014001.
[20] A. Fridman, S. Nester, L.A. Kennedy, A. Saveliev, O.M. Yardimci, Gliding arc gas discharge, Prog Energ Combust 25 (1999) 211-231.
[21] J.J. Zhu, J.L. Gao, Z.S. Li, A. Ehn, M. Aldén, A. Laesson, Y. Kusano, Sustained diffusive alternating current gliding arc discharge in atmospheric pressure air, Appl Phys Lett 105 (2014) 234102.
[22] W.Z. Wang, A. Berthelot, S. Kolev, X. Tu, A. Bogaerts, CO_2 conversion in a gliding arc plasma: 1D cylindrical discharge model, Plasma Sources Sci T 25 (2016) 065012.
[23] J.J. Zhu, A. Ehn, J.L. Gao, C.D. Kong, M Aldén, M. Salewski, F. Leipold, Y. Kusano, Z.S. Li, Translational, rotational, vibrational and electron temperatures of a gliding arc discharge, Opt Express 25 (2017) 20243-20257.
[24] R. Snoeckx, A. Bogaerts, Plasma technology-a novel solution for CO_2 conversion?, Chem Soc rev 46 (2017) 5805-5863.
[25] A. Fridman, Plasma chemistry, Cambridge University Press, New York, 2008.
[26] A. Gutsol, A. Rabinovich, A. Fridman, Combustion-assisted plasma in fuel conversion, J Phys D Appl Phys 44 (2011) 274001.
[27] J.J. Zhu, J.L. Gao, A. Ehn, M. Aldén, Z.S. Li, D. Moseec, Y. Kusano, M. Salewski, A.Alpers, P. Gritzmann, M. Schwenk, Measurements of 3D slip velocities and plasma column lengths of a gliding arc discharge, Appl Phys Lett 106 (2015) 041602.
[28] Kozák, Tomáš, Bogaerts A. Aldén, Z.S. Li, D. moseev, Y. Kusano, M. Salewski, A. Alpers, P. Gritzmann, M. Schwenk, Splitting of CO_2 by vibrational excitation in non-equilibrium plasmas: a reaction kinetics model, Plasma Sources Sci T 23 (2014) 045004.
[29] A. Indarto, D.R. Yang, J.W. Choi, H. Lee, H.K. Song, Gliding arc plasma processing of CO_2 conversion, J Hazard Mater 146 (2007) 309-315.
[30] S.C. Kim, Y.N. Chun, Development of a gliding arc plasma reactor for CO_2 destruction, Environ Technol 35 (2014) 2940-2946.
[31] S.C. Kim, M.S. Lim, Y.N. Chun. Reduction characteristics of carbon dioxide using a plasmatron, Plasma Chem Plasma P 34 (2014) 125-143.
[32] J.J. Zhu, Z.W. Sun, Z.S. Li, A. Ehn, M. Aldén, M. Salewski, F. Leipold, Y. Kusano, Dynamics, OH distributions and UV emission of a gliding arc at various flow-rates investigated by optical measurements, J Phys D Appl Phys 47 (2014) 295203.
[33] A. Indarto, J.W. Choi, H. Lee, H.K. Song, N. Coowanitwong, Discharge characteristics of a gliding-arc plasma in chlorinated methanes diluted in atmospheric air, Plasma Devices Oper 14 (2006) 15-26.
[34] O. Taylan, H. Berberoglu. Dissociation of carbon dioxide using a microhollow cathode discharge plasma reactor: effects of applied voltage, flow rate and

concentration, Plasma Sources Sci T 24 (2015) 015006.

[35] M. Ramakers, G. Trenchev, S. Heijkers, W. Wang, A. Bogaerts, Gliding arc plasmatron: Providing an alternative method for carbon dioxide conversion, Chemsuschem 10 (2017) 2642-2652.

[36] D.H. Mei, X. Tu, Atmospheric pressure non-thermal plasma activation of CO_2 in a packed-bed dielectric barrier discharge reactor, Chemphyschem 18 (2017) 3253-3259.

[37] S. Paulussen, B. Verheyde, X. Tu, C.D. Bie, T. Martens, D. Petrovic, A. Bogaerts, B. Sels, Conversion of carbon dioxide to value-added chemicals in atmospheric pressure dielectric barrier discharges, Plasma Sources Sci T 19 (2010) 34015-34016.

[38] A. Ozkan, A. Bogaerts, F. Reniers, Routes to increase the conversion and the energy efficiency in the splitting of CO_2 by a dielectric barrier discharge, J Phys D Appl Phys 50 (2017) 084004.

[39] O. Taylan, H. Berberoglu, Dissociation of carbon dioxide using a microdischarge plasma reactor, ASME 2013 international mechanical engineering congress and exposition, 2015.

[40] M.S. Bak, S.K. Im, M. Cappelli, Nanosecond-pulsed discharge plasma splitting of carbon dioxide, IEEE T Plasma Sci 43 (2015) 1002-1007.

[41] L.T. Hsieh, W.J. Lee, C.T. Li, C.Y. Chen, Y.F. Wang, M.B. Chang, Decomposition of carbon dioxide in the RF plasma environment, J Chem Technol Biot 73 (1998) 432-442.

[42] W. Tsang, R. Hampson, Chemical kinetic data base for combustion chemistry. Part I. Methane and related compounds, Journal of Physical and Chemical Reference Data, 15 (1986) 1087-1279.

[43] F. Saleem, K. Zhang, A. Harvey. Role of CO_2 in the conversion of toluene as a tar Surrogate in a nonthermal plasma dielectric barrier discharge reactor, Energ Fuels 32 (2018) 5164–5170.

[44] A.J. Wu, H. Zhang, X.D. Li, S.Y. Lu, C.M. Du, J.H. Yan, Determination of spectroscopic temperatures and electron density in rotating gliding arc discharge, IEEE T Plasma Sci 43 (2015) 836-845.

[45] Y.N. Chun, S.C. Kim, K. Yoshikawa. Decomposition of benzene as a surrogate tar in a gliding arc plasma, Environ Prog Sustain 32 (2013) 837-845.

[46] S.R. Sun, H.X. Wang, D.H. Mei, X. Tu, A. Bogaerts, CO_2 conversion in a gliding arc plasma: Performance improvement based on chemical reaction modeling, J CO_2 Util 17 (2017) 220-234.

[47] G.J. van Rooij, D.C.M. van den Bekerom, N. den Haeder, T. Minea, G. Berden, W.A. Bongers, R. Engeln, M.F. Graswinckel, E. Zoethout, M.C.M. van de Danden, Taming microwave plasma to beat thermodynamics in CO_2 dissociation, Faraday Discuss 183 (2015) 233-248.

[48] M. Leins, S. Gaiser, J. Kopecki, W.A. Bongers, A. Goede, M.F. Graswinckel, A. Schulz, M. Walker, M.C.M van de Sanden, T. Hirth, Dissociation of CO_2 by means of a microwave plasma process for solar fuels production, 22nd international symposium on plasma chemistry, 2015.

[49] W. Xu, M.W. Li, G.H. Xu, Y.L. Tuan, Decomposition of CO_2 Using DC Corona Discharge at Atmospheric Pressure, Jpn J Appl Phys 43 (2004) 8310-8311.
[50] R. Aerts, W. Somers, A. Bogaerts, Carbon dioxide splitting in a dielectric barrier discharge plasma: a combined experimental and computational study, Chemsuschem 8 (2015) 702-716.
[51] Q.Q. Yu, M. Kong, T. Liu, J.H. Fei, X.M. Zheng, Characteristics of the Decomposition of CO_2 in a Dielectric Packed-Bed Plasma Reactor, Plasma ChemPlasma P 32(2012) 153-163.
[52] D.H. Mei, X. Tu, Conversion of CO_2 in a cylindrical dielectric barrier discharge reactor: Effects of plasma processing parameters and reactor design, J CO_2 Util 19 (2017) 68-78.
[53] I. Belov, S. Paulussen, A. Bogaerts, Appearance of a conductive carbonaceous coating in a CO_2 dielectric barrier discharge and its influence on the electrical properties and the conversion efficiency[J]. Plasma Sources Sci T 25 (2016) 015023.
[54] Y. Nigara, B. Cales. ChemInform Abstract: Production of Carbon Monoxide by Direct Thermal Splitting of Carbon Dioxide at High Temperature, Cheminform 17 (1986).
[55] S.S. Xu, S.S. Li, W.T. Yao, D.H. Dong, K. Xie, Direct electrolysis of CO_2 using an oxygen-ion conducting solid oxide electrolyzer based on $La_{0.75}Sr_{0.25}Cr_{0.5}Mn_{0.5}O_{3-\delta}$ electrode, J Power Sources 230 (2013) 115-121.
[56] B.W. Wang, Q.M. Sun, Y.J. Lü, M.L. Yang, W.J. Yan, Steam reforming of dimethyl ether by hliding arc gas discharge plasma for hydrogen production, Chinese J Chem Eng 22 (2014) 104-112.
[57] S.C. Kim, Y.N. Chun, Development of a gliding arc plasma reactor for CO_2 destruction, Environ Technol 35 (2014) 2940-6.